Stochastic resonance in Hopfield neural networks for transmitting binary signals

Lingling Duan [a], Fabing Duan [a,*], François Chapeau-Blondeau [b], Derek Abbott [c]

[a] *Institute of Complexity Science, Qingdao University, Qingdao 266071, PR China*
[b] *Laboratoire Angevin de Recherche en Ingénierie des Systèmes (LARIS), Université d'Angers, 62 avenue Notre Dame du Lac, 49000 Angers, France*
[c] *Centre for Biomedical Engineering (CBME) and School of Electrical & Electronic Engineering, The University of Adelaide, Adelaide, SA 5005, Australia*

ARTICLE INFO

ABSTRACT

We investigate the stochastic resonance phenomenon in a discrete Hopfield neural network for transmitting binary amplitude modulated signals, wherein the binary information is represented by two stored patterns. Based on the potential energy function and the input binary signal amplitude, the observed stochastic resonance phenomena involve two general noise-improvement mechanisms. A suitable amount of added noise assists or accelerates the switch of the network state vectors to follow input binary signals more correctly, yielding a lower probability of error. Moreover, at a given added noise level, the probability of error can be further reduced by the increase of the number of neurons. When the binary signals are corrupted by external heavy-tailed noise, it is found that the Hopfield neural network with a large number of neurons can outperform the matched filter in the region of low input signal-to-noise ratios per bit.

© 2019 Elsevier B.V. All rights reserved.

1. Introduction

The concept of stochastic resonance, proposed by Benzi [1] in bistable physical models [2–4], expresses the possibility for random noise to activate the interwell transitions between the minima of the potential energy and in this way improve the synchronized response to a weak periodic signal. Gradually, the phenomenon of stochastic resonance was observed and extended to aperiodic signals [5] and suprathreshold (non-weak) signals [6, 7], and various models, wherein the noise-enhanced effect occurs, evolved from a single system [3,4,8–11], parallel or coupled nonlinear subsystems [5,6,12–14], neural networks [15–21], to complex systems [22–26]. Among these studies, the constructive role of noise in Hopfield neural networks [28–37] attacks the greatest attention. Schonfeld [15] first found that the presence of a mild noise level can improve the performance of the noisy Hopfield neural network characterized by the probability of error. Motivated by perceptual bistability involved in the interpretation of ambiguous figures, Riani and Simontto [16] observed that the Hopfield neural network exhibits a maximum signal-to-noise ratio (SNR) at a non-vanishing optimum noise level in the framework of stochastic resonance [1,4]. Beyond the deterministic periodic stochastic resonance effects in a recurrent neural network with Hopfield-type

memory [18], Katada and Nishimura [38] explored the effective responses of the double-well or multi-well model to the aperiodic signals stored by different patterns. Given fixed connection weights and topology of networks, Pavlović et al. [39] showed that, based on the stability intervals associated with the desired and undesired states, the "Bad-Good" error of the binary Hopfield neural network can be enhanced for an optimal range of noise levels. Actually, the application of Hopfield neural networks to signal transmission has been adequately investigated as a suboptimal scheme at a lower computational cost [41–44].

In this paper, we investigate the stochastic resonance effect in a discrete Hopfield network for transmitting binary amplitude modulated signals, as shown in Fig. 1. The considered Hopfield neural network stores two *N*-dimensional fundamental memory vectors as patterns to be memorized, and the synaptic weight matrix *W* of the network is defined by the outer-product of the two stored patterns [27,28]. The binary digits are mapped onto the stored patterns with a weak modulated amplitude in a finite bit interval. Without the added noise components in each neuron, the network state vector cannot develop into the corresponding attraction basins established by the fundamental memory vectors, because the modulated amplitude is too weak or the bit interval is too short. Under these circumstances, the decoded scheme will yield error bits, and the probability of bit error of the Hopfield neural network is considerably high. When a suitable amount of noise is added into each neuron, it is observed that the net-
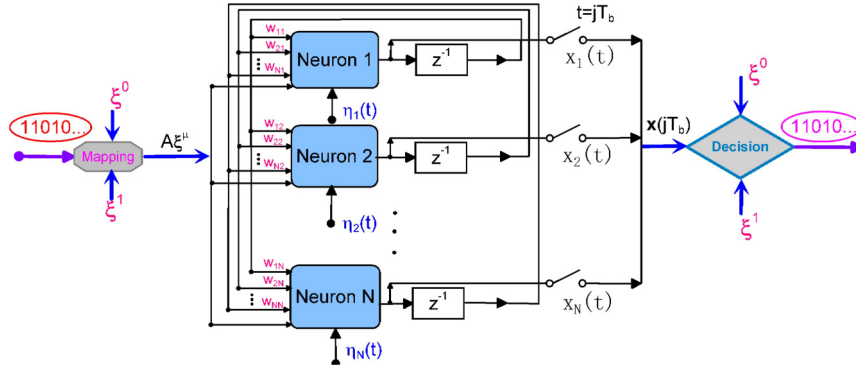
Fig. 1. Block diagram representation of a discrete Hopfield neural network with synaptic noise components $\eta_i(t)$ in the ith neuron for transmitting binary signals represented by two stored patterns ξ^0 and ξ^1. Here, A is the modulated amplitude, T_b is the bit interval, and z^{-1} indicates the function of a unit delay.

work state vector can reach the attraction basins associated with the stored patterns, resulting in a much lower probability of bit error. This typical behavior of stochastic resonance effect in a discrete Hopfield neural network for transmitting binary signals will be investigated in detail. Moreover, as the number of neurons in the network increases, the probability of error of the network can be further lowered at a given added noise level. Another situation is when the binary amplitude modulated signal is already corrupted by external noise, and the prior information of binary digits is lost. In this situation, we can map the bipolar amplitude modulated signals onto the fundamental memory vector and its inverted (spurious) vector to the network. Under this condition, we also compare the performance of the Hopfield neural network with that of the matched filter for decoding the binary information, especially in certain external heavy-tailed non-Gaussian noisy environments.

2. Discrete Hopfield network model

Consider a discrete Hopfield neural network model consisting of N mutually connected neurons, as shown in Fig. 1. Let $x_i(t)$ denote the state of the neuron i at the time t, and the N neurons are assumed to be updated synchronously at the next time $t + 1$ as [18,28,38]

$$x_i(t+1) = \tanh[\beta(v_i(t) + s_i(t) + \eta_i(t))], \quad (1)$$

where β is the slope parameter, the local field $v_i(t) = \sum_{j=1}^{N} w_{ij}x_j(t) - \theta_i$, the synaptic weight from neuron i to neuron j is w_{ij}, θ_i is the activity threshold of the neuron i, the input signal is $s_i(t)$ and the mutually independent synaptic noise components $\eta_i(t)$ are with zero mean and the same variance σ_η^2 for $i, j = 1, 2, \cdots, N$, as shown in Fig. 1. Then, the network state vector is given by $\mathbf{x}(t) = [x_1(t), x_2(t), \cdots, x_N(t)]^\top$. Since the state x_i satisfies $-1 \leq x_i \leq 1$ in Eq. (1), then $N \times 1$ dimensional fundamental memory vectors $\xi^\mu(\mu = 0, 1)$, as stored patterns to be memorized by the network, have the ith element $\xi_i^\mu = \pm 1$.

We randomly choose the two patterns $\xi^\mu(\mu = 0, 1)$ out of the 2^N possible patterns, and suppose the two stored patterns ξ^0 and ξ^1 are almost orthogonal [27,28,40], i.e.

$$\frac{1}{N}(\xi^0)^\top \xi^1 \simeq 0. \quad (2)$$

Then, according to Hebb's rule of the outer product [27,28], we construct the $N \times N$ synaptic-weight matrix

$$\mathbf{W} = \frac{1}{N} \sum_{\mu=0}^{1} \xi^\mu (\xi^\mu)^\top \quad (3)$$

with w_{ij} as its ij-th element.

As in Fig. 1, the information-carrying digits 0 and 1 with prior probabilities $P(0)$ and $P(1)$, respectively, are modulated as the patterns $A\xi^0$ and $A\xi^1$ that last over the time intervals $jT_b \leq t < (j+1)T_b$ for $j = 0, 1, 2, \cdots$. Here, A is the modulated amplitude and T_b is the bit interval. Define the potential energy function of the Hopfield neural network as

$$e(\mathbf{x}) = \frac{1}{2}\mathbf{x}(t)^\top \mathbf{W}\mathbf{x}(t) - \frac{1}{\beta}\sum_{i=1}^{N} \ln\Big[\cosh\beta\big(\mathbf{W}\mathbf{x}(t) - \theta + A\xi^\mu\big)\Big] \quad (4)$$

with the threshold vector $\theta = [\theta_1, \theta_2, \cdots, \theta_N]^\top$. The potential energy function of Eq. (4) has one global minimum or multiple local minima of the energy that correspond to the equilibria of the network state vector $\mathbf{x}$. Setting $\partial e(\mathbf{x})/\partial \mathbf{x}$ to be zero and for sufficiently large time steps, we can find the equilibria $\mathbf{x}^*$ by the nonlinear equation

$$\mathbf{x}^*(T) = \tanh[\beta(\mathbf{W}\mathbf{x}^*(T) - \theta + A\xi^\mu)]$$

for $\mu = 0$ or 1. For instance, consider the network consisting of $N = 2$ neurons, and the two stored patterns are taken as $\xi^0 = [1, 1]^\top$ and $\xi^1 = [1, -1]^\top$. It is seen in Fig. 2 (a) that, for the modulated amplitude $A = 0.02$ and the slope parameter $\beta = 1.2$, the potential energy function $e(\mathbf{x})$ has three local minima and one global minimum. Here, the modulated binary signal is taken as $A\xi^1$ and holds for a sufficiently large time. In this case, there are four equilibria $\mathbf{x}^*$ that locate at the valley bottoms, as shown in Fig. 2 (a). Correspondingly, the modulated amplitude $A = 0.02$ is said to be subthreshold in agreement with the mechanism of stochastic resonance. Given an initial state vector $\mathbf{x}(0)$ and without the assistance of noise, the network state vector $\mathbf{x}$ will converge to the corresponding equilibrium that captures the initial vector $\mathbf{x}(0)$. For instance, for trajectories 1 and 2, as the time step t increases, the network state vectors $\mathbf{x}$ start from two initial vectors $\mathbf{x}(0)$, and approach different equilibria $\mathbf{x}^{*,1} = [-0.6076, -0.6956]^\top$ and $\mathbf{x}^{*,2} = [0.6956, -0.6956]^\top$, respectively, as shown in Fig. 2 (a). When the modulated amplitude $A = 0.1$, the potential energy function has only one global minimum, as shown in Fig. 2 (b). In this case, the modulated amplitude A is suprathreshold. For different initial vectors $\mathbf{x}(0)$, network state vectors $\mathbf{x}$ approach the same equilibrium $\mathbf{x}^* = [0.7876, -0.7876]^\top$ (see trajectories 3 and 4), as the evolution of the network state vector lasts for quite a long time. Therefore, the potential energy function in Eq. (4) of the Hopfield neural network is analogous to that of the bistable system [1,4], and as we are going to show the occurrence possibility of noise-improved effects for transmitting binary signals.

During this signal transmission process, there are two important problems that need to be solved: one is the network state
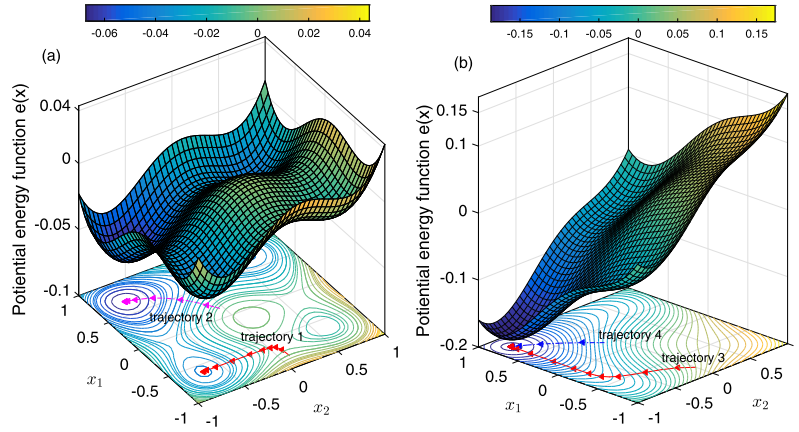
Fig. 2. Potential energy function $e(\mathbf{x})$ of a Hopfield neural network with $N = 2$ neurons for the modulated binary signal $A\xi^1$ with (a) the subthreshold amplitude $A = 0.02$, (b) the suprathreshold amplitude $A = 0.1$, the slope parameter $\beta = 1.2$ and all activity thresholds $\theta_i = 0$. The color bar represents the value of $e(\mathbf{x})$. (For interpretation of the colors in the figure(s), the reader is referred to the web version of this article.)
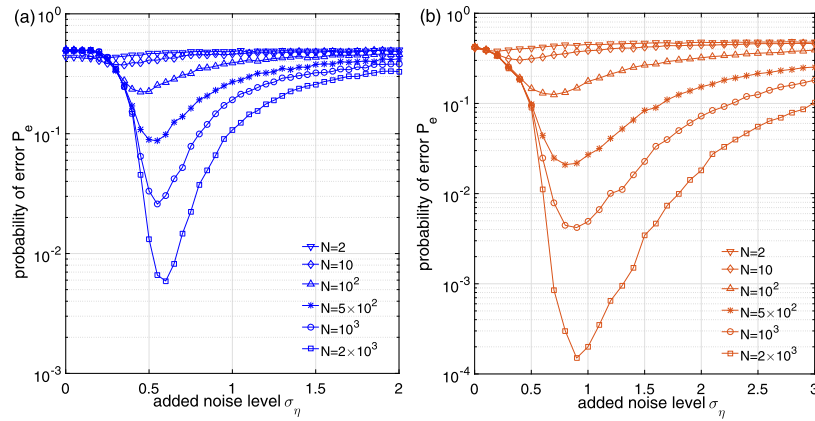

Fig. 3. Probability of error P_e in Eq. (8) as a function of the added noise level σ_η for N neurons in the Hopfield neural network with (a) the subthreshold amplitude $A = 0.02$ and the bit interval $T_b = 10$, and (b) the suprathreshold amplitude $A = 0.1$ and the bit interval $T_b = 3$. The added noise $\eta_i(t)$ are mutually independent of each other and accord to the zero-mean Gaussian distribution. Other parameters are the same as in Fig. 2.

vector $\mathbf{x}(t)$ might not approach the expected pattern ξ^μ for subthreshold (weak) modulated signals, because the equilibria $\mathbf{x}^*$ are multiple, as illustratively shown in Fig. 2 (a). The other one is that, even as the modulated amplitude A is non-weak (suprathreshold) (e.g. see Fig. 2 (b)), $\mathbf{x}(t)$ does require a sufficiently large time t to converge to the sole equilibrium of $\mathbf{x}^*$, and can not switch correctly to follow the variety of input signals in a finite bit interval T_b. To answer these questions, a quantity of the overlap between the network state vector $\mathbf{x}(t)$ and the stored pattern ξ^μ is defined as

$$m_\mu(t) = \frac{1}{N}\mathbf{x}(t)^\top \xi^\mu \qquad (5)$$

to measure how $\mathbf{x}(t)$ is close to the stored pattern ξ^μ for $\mu = 0$ and 1. From Eq. (5), the N-dimensional space V of the state vector $\mathbf{x}(t)$ can be divided into two subsets V_0 and V_1 as

$$V_0 = \{\mathbf{x}|m_0(t) \geq m_1(t)\}, \ V_1 = \{\mathbf{x}|m_0(t) < m_1(t)\}, \qquad (6)$$

where V_0 indicates the attraction basin of the stored pattern ξ^0, conversely for V_1. As in Fig. 2, when the modulated pattern $A\xi^\mu$ is fed into the network, the network state vectors $\mathbf{x}(t)$ will, in the statistical sense, mainly fall into the attraction basin V_μ that depends on $A\xi^\mu$ for $\mu = 0, 1$. Then, at the sampling times $t = jT_b$ for $j = 1, 2, \cdots$ and due to the mutually orthogonal stored patterns ξ^μ, we can decode binary digits by observing which subset

V_μ the network state vector $\mathbf{x}(t)$ falls into. It is equivalent to compute the overlaps $m_\mu(jT_b)$ of Eq. (5) to decode binary digits as

$$m_0(jT_b) \underset{1}{\overset{0}{\gtrless}} m_1(jT_b). \qquad (7)$$

Using this decision rule of Eq. (7), we have the decoded binary digits and the probability of error

$$P_e = P(0)P(1|0) + P(1)P(0|1), \qquad (8)$$

where the probability of error bits $P(1|0)$ denotes the decoded digit to be 1 when the input digit is 0, and conversely for $P(0|1)$. We will find that the addition of a suitable amount of noise will induce or expedite the convergence process of $\mathbf{x}(t)$ into the subset V_μ, resulting in a nonmonotonic behavior of the probability of error P_e explained as the stochastic resonance effect in Hopfield neural networks.

3. Stochastic resonance effects in Hopfield neural networks

Fig. 3 shows the behaviors of the probability of error P_e in Eq. (8) as a function of the added noise level σ_η for N neurons in the Hopfield network. For both subthreshold (weak) amplitude $A = 0.02$ and suprathreshold (non-weak) amplitude $A = 0.1$, it is seen in Figs. 3 (a) and (b) that, as the added noise level σ_η increases, the probability of error P_e gradually decreases to a minimum at an optimal but non-zero level of σ_η, and then increases for
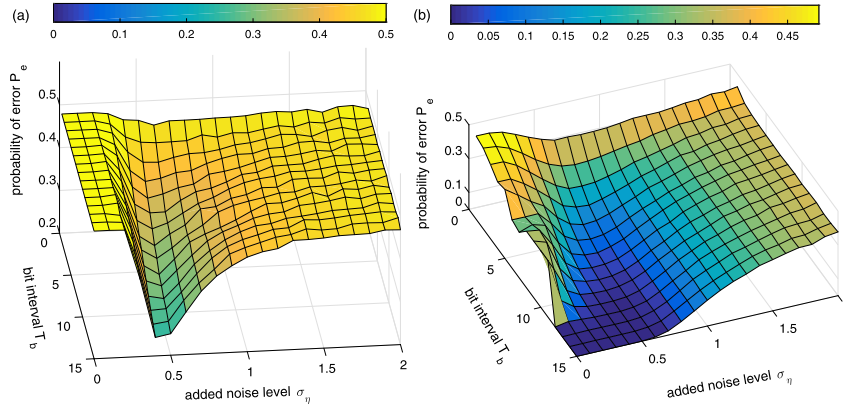
Fig. 4. Probability of error P_e as a function of parameters (T_b, σ_η) for (a) the subthreshold amplitude $A = 0.02$ and (b) the suprathreshold amplitude $A = 0.1$ in the Hopfield neural network with $N = 50$ neurons. The color bar represents the value of P_e. The added noise and other parameters are the same as in Fig. 2.
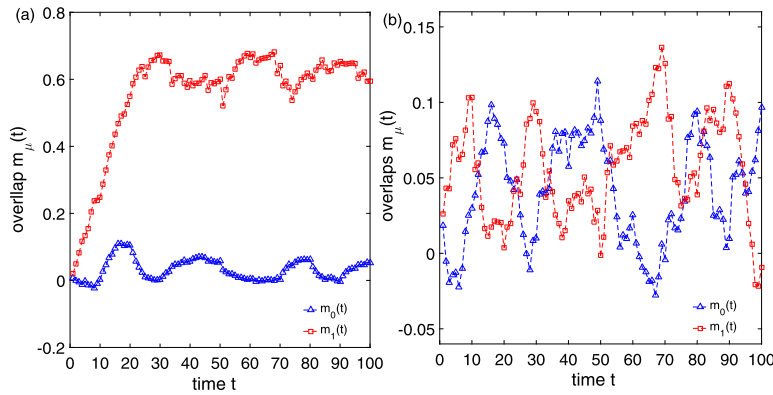

Fig. 5. Overlap $m_\mu(t)$ for the subthreshold amplitude $A = 0.02$ and bit interval $T_b = 10$ at added noise levels (a) $\sigma_\eta = 0$ and (b) $\sigma_\eta = 0.6$. Other parameters are the same as in Fig. 2.

large noise levels. This is the stochastic resonance effect in Hopfield neural networks that occurs for both weak and non-weak modulated amplitudes. Moreover, as the neuron number N increases, the minimum of P_e obtained at the optimal noise level also gradually decreases. The reason is that, under this condition, the transmission power $\varepsilon = NA^2 T_b$ of the binary signal and the input SNR per bit $NA^2 T_b / \sigma_\eta^2$ also increase with the neuron number N. Thus, it is seen in Fig. 3 that the Hopfield neural network with larger neuron number N presents a lower probability of error P_e at a given added noise level σ_η.

However, when the bit interval T_b varies, the probability of error P_e will exhibit different behaviors for subthreshold and suprathreshold modulated amplitudes. Fig. 4 illustrates the results of P_e in Eq. (8) as a function of the bit interval T_b and the added noise level σ_η for amplitudes $A = 0.02$ and 0.1 in the Hopfield neural network with $N = 50$ neurons. It is seen in Fig. 4 (a) that, upon the increase of bit interval T_b, the minimum probability of error P_e decreases due to the increased transmission power $\varepsilon = NA^2 T_b$. But, no matter how long the bit interval T_b is, the probability of error P_e at the added noise level $\sigma_\eta = 0$ is always about 0.5. For the suprathreshold amplitude $A = 0.1$, it is shown in Fig. 4 (b) that there is a critical bit interval $T_b^c = 12$. When the bit interval $T_b \geq T_b^c$, the initial probability error P_e at $\sigma_\eta = 0$ is zero. These interesting results will be interpreted as follows.

From the observations in Figs. 4 (a) and (b), we argue that the stochastic resonance effect contains the classical mechanism of an amplitude effect, in which a small input signal receives assistance from noise to reach the assigned attraction basin of the network. This explanation can be further explained by Fig. 5 (a) for $N = 2 \times 10^3$ neurons in a Hopfield neural network. For the

subthreshold modulated amplitude $A = 0.02$ and without the addition of noise, as shown in Fig. 5 (a), the overlap $m_1(t)$ is always larger than the overlap $m_0(t)$, because the network state vector $\mathbf{x}(t)$ always falls into the subset V_1 that is the attraction basin of the stored pattern $\boldsymbol{\xi}^1$. Without the help of noise ($\sigma_\eta = 0$), the network state vector $\mathbf{x}(t)$ can not escape from this attraction basin and then we obtain the overlap inequality $m_1(jT_b) \geq m_0(jT_b)$. This inequality does not vary at each sampling times $t = jT_b$, and leads to one half error digits and the probability of error $P_e \approx 0.5$ at $\sigma_\eta = 0$, even the input modulated signal $A\boldsymbol{\xi}^1$ lasts for a longer bit interval T_b (see Fig. 4 (a)). It is seen in Fig. 5 (b) that, at an optimal added noise level $\sigma_\eta = 0.6$, the overlap $m_\mu(t)$, assisted by the added noise, alternates over time according to the modulated vectors $A\boldsymbol{\xi}^\mu$ for $\mu = 0$ and 1. Although the addition of noise to the network randomizes the output states of neurons and reduces the values of $m_\mu(t)$, it forms improved decision according to the overlap inequalities $m_1(jT_b) \gtrless m_0(jY_b)$ of Eq. (7), leading to an improved probability of error P_e, as shown in Fig. 3 (a).

Furthermore, the stochastic resonance effect is also a temporal effect, as shown in Fig. 3 (b), in which a non-weak input signal receives assistance from noise to switch correctly to follow the variability of the binary information carried in each of the successive bit intervals. This explanation is illustrated in Fig. 6 for a Hopfield neural network with $N = 2 \times 10^3$ neurons. For the suprathreshold amplitude $A = 0.1$ and without the added noise ($\sigma_\eta = 0$), the output state vector of the network can not reach the attraction basin that corresponds to the modulated vector $A\boldsymbol{\xi}^\mu$ in such a short bit interval of $T_b = 3$, as shown in Fig. 6 (a). Specially, at time $t = 15$, two same digits 0 join together and the state vector of the network $\mathbf{x}(t)$ is much closer to the modulated vector $A\boldsymbol{\xi}^0$, rather than $A\boldsymbol{\xi}^1$.
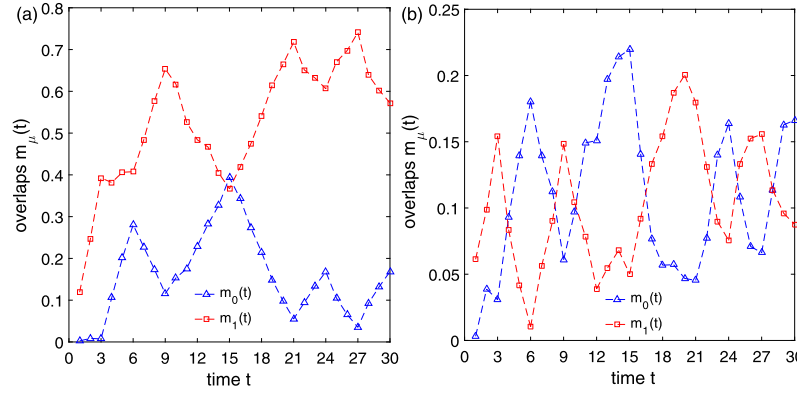
Fig. 6. Overlap $m_\mu(t)$ for the suprathreshold amplitude $A = 0.1$ and bit interval $T_b = 3$ at added noise levels (a) $\sigma_\eta = 0$ and (b) $\sigma_\eta = 0.9$. Other parameters are the same as in Fig. 2.

Besides this special case, the overlaps almost accord with the relation $m_1(jT_b) \geq m_0(jT_b)$, and the probability of error P_e is usually larger. When an optimal amount of noise ($\sigma_\eta = 0.9$) is added to the network, the overlaps $m_\mu(t)$, accelerated by the added noise, will capture the variability of input binary modulated vectors $A\boldsymbol{\xi}^\mu$ more correctly in each bit interval T_b, as shown in Fig. 6 (b). Therefore, the probability of error P_e is much lower at the optimal noise level $\sigma_\eta = 0.9$, as indicated in Fig. 3 (b). It is also noted that, for a sufficient large bit interval T_b and without the added noise $\sigma_\eta = 0$, the output state vector $\mathbf{x}(t)$ of the network can reach the attraction basin that corresponds to the modulated vector $A\boldsymbol{\xi}^\mu$, and the overlaps accord well with the relation $m_1(jT_b) \geq m_0(jT_b)$, as shown in Fig. 4 (b). In this case, the addition of noise to neurons is unnecessary. Of course, for both modulated amplitudes $A = 0.02$ and 0.1, too much added noise will completely randomize the overlaps $m_\mu(t)$ and results in the wrong relation $m_1(jT_b) \gtrless m_0(jT_b)$. Then, for a large added noise level σ_η, the decoding rule yields more digits decoded in error and a higher probability of error P_e, as shown in Figs. 3 and 4.

In practice, we often encounter such a situation: the information-carrying digits 0 and 1 are mapped on the bipolar pulse-amplitude modulated waveforms $-A$ or $+A$ in each bit interval, but are corrupted by external white noise $\upsilon(t)$ with the standard derivation σ_υ. Under this circumstance, the noisy input becomes $I(t) = \pm A + \upsilon(t)$ and the prior information of digits represented by $\pm A$ is hidden by the noise. Thus, two selected patterns $\boldsymbol{\xi}^1$ and $\boldsymbol{\xi}^0$ cannot be assigned to the modulated amplitudes $\pm A$. Fortunately, when the neuron thresholds $\theta_i = 0$, the spurious state vectors $-\boldsymbol{\xi}^\mu$ are also stable [27,28]. This conclusion can be also demonstrated by replacing $\boldsymbol{\xi}^\mu$ and $\mathbf{x}(t)$ with $-\boldsymbol{\xi}^\mu$ and $-\mathbf{x}(t)$ in Eqs. (1) and (4). This also inspires us to reform the decoding scheme in Fig. 1 as follows: mapping digits 0 onto $-A\boldsymbol{\xi}^\mu$ and digits 1 onto $+A\boldsymbol{\xi}^\mu$, wherein the decision rule of Eq. (7) is still applicable. For instance, we take the modulated amplitude $A = 0.1$, the bit interval $T_b = 4$ and the standard derivation of the external Gaussian noise $\upsilon(t)$ is $\sigma_\upsilon = 0.1$. Then, the input SNR per bit of the noisy input $I(t)$ can be calculated as $R_{\text{in}} = 10\log_{10}(A^2 T_b/\sigma_\upsilon^2) = 6.02$ dB. It is seen in Fig. 7 that, as the added noise level σ_η increases, the probability of error P_e also has a minimum at an optimal non-zero value of σ_η for different numbers N of neurons. The addition of noise to the network is still useful to the improvement of the probability of error at a non-zero optimal noise level. However, due to the external noise $\upsilon(t)$, the initial input SNR per bit R_{in} is given. Then, the probabilities of error P_e approach to each other asymptotically for very large neuron numbers N, as shown in Fig. 7 (e.g. $N = 10^3$ and 2×10^3), even with the help of the added noise $\eta(t)$.

From the above analysis of the probability of error, we note that the Hopfield neural network can be viewed as a receiver for
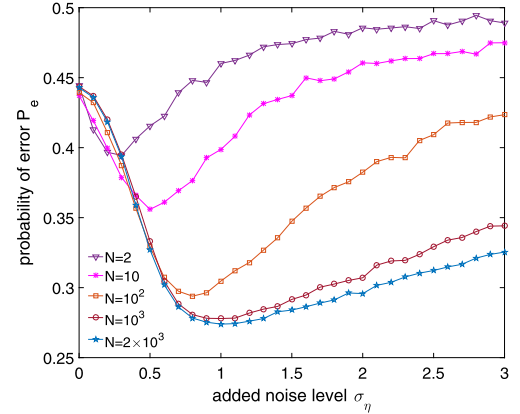

Fig. 7. Probability of error P_e versus the added noise level σ_η for different neurons numbers N. Here, the modulated amplitude $A = 0.1$, the bit interval $T_b = 4$, and the standard derivation of external noise is $\sigma_\upsilon = 0.1$. Other parameters are the same as in Fig. 2 (b).

decoding the transmitted binary signals. On the other hand, for detecting a known signal in additive white Gaussian noise, it is well known that the optimal detector is the matched filter or linear correlation receiver given by

$$\sum_{n=jT_b}^{(j+1)T_b} AI(t) \underset{0}{\overset{1}{\gtrless}} \sum_{n=jT_b}^{(j+1)T_b} -AI(t), \tag{9}$$

with the probability of error defined by

$$P_e = Q\left(\sqrt{R_{\text{in}}}\right) = Q\left(\sqrt{A^2 T_b/\sigma_\upsilon^2}\right), \tag{10}$$

where $Q(x) = \int_x^\infty \exp(-t^2/2)/\sqrt{2\pi}\,dt$ [45]. Due to its simplicity for both practical implementation and theoretical analysis, the matched filter is very often exploited for detection, even when it is no longer optimal for detecting known signals in non-Gaussian noise. For these reasons the matched filter represents a meaningful reference that we shall use for comparison with the Hopfield neural networks under study. Specifically, consider the generalized Gaussian noise $\upsilon(t)$ with its distribution $f_\upsilon(x) = c_1 \exp\left(-c_2 |x/\sigma_\upsilon|^\alpha\right)/\sigma_\upsilon$, where the exponent $\alpha > 0$, $c_1 = \frac{\alpha}{2}\Gamma^{\frac{1}{2}}(\frac{3}{\alpha})/\Gamma^{\frac{3}{2}}(\frac{1}{\alpha})$, $c_2 = [\Gamma(\frac{3}{\alpha})/\Gamma(\frac{1}{\alpha})]^{\frac{\alpha}{2}}$, and $\Gamma(x)$ is the gamma function [45]. This non-Gaussian noise model is often used to mimic practical noisy environments wherein signals and systems are operated. As the exponent α varies, we can conveniently consider a spectrum of densities ranging from the Gaussian ($\alpha = 2$) to those with relatively much faster ($\alpha > 2$) or slower ($\alpha < 2$) rates of exponential decay of their tails [46]. For a given R_{in}, we add N
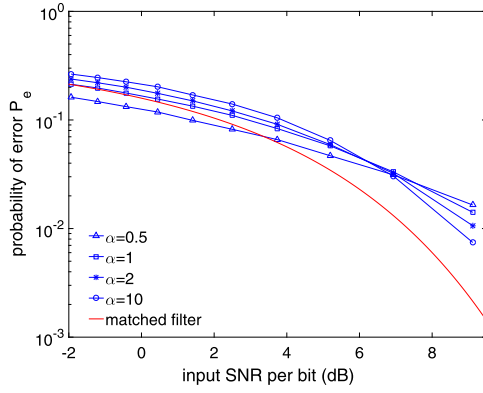
Fig. 8. Minimum probability of error P_e of the Hopfield network with 2×10^3 neurons as a function of the input SNR per bit $R_{\text{in}} = 10\log_{10}(A^2 T_b/\sigma_v^2)$. For comparison, the probability of error P_e of the matched filter is also plotted. Other parameters are the same as in Fig. 7.

mutually independent Gaussian noise $\eta_i(t)$ into the Hopfield neural network with N neurons, and tune the added noise level σ_η optimally to obtain the minimum probability of error P_e, as shown in Figs. 3 and 7. For different noise types of $\upsilon(t)$ with exponents $\alpha = 0.5, 1, 2$ and 10, the minimum probability of error P_e is plotted as a function of the input SNR per bit R_{in}. For comparison, the probability of error P_e of the matched filter in Eq. (10) is also plotted. It is seen in Fig. 8 that, for $\alpha = 0.5$, the Hopfield neural network, compared with the matched filter, provides a lower probability of error as the input SNR per bit is less than 3 dB. This comparison results demonstrate the superiority of the Hopfield neural network with a large number of neurons for transmitting the binary signals buried in the heavy-tailed background noise $\upsilon(t)$ ($\alpha = 0.5$). Thus, we expect that the performance of the Hopfield neural network is worthy of being further studied for more rigorous noisy environments.

4. Conclusion

In this paper, we study stochastic resonance effects in a discrete Hopfield neural network for transmitting binary amplitude modulated signals. The potential energy function of the Hopfield neural network, similar to that of the well-known bistable system model, has multiple minima or only one minimum that is determined by the built-in stored patterns of the network. Thus, stochastic resonance effects in a discrete Hopfield neural network involve two general mechanisms: When the amplitude is small, the network state vectors, in the statistical sense, converge to the minimum equilibria with the help of added noise, leading to an improved probability of error. For modulated signals with large amplitudes, it is found that the addition of noise into the neurons of the network can accelerate the convergence process of the network state vector, and makes the network state vectors switch more correctly to follow the variability of the binary signal in successive bit intervals. In addition, when the bipolar binary amplitude modulated signals are corrupted by the external noise, the designed transmission scheme of discrete Hopfield neural networks is also valid by mapping binary digits onto one stored pattern and its spurious state. Finally, we discuss the performance improvement of Hopfield neural networks in the heavy-tailed non-Gaussian noise background.

Some interesting open questions arise. For instance, the multistability and mono-stability of the potential energy function depend on a critical amplitude A_c that needs to be theoretically determined. We also note that the binary information here is carried in the two stored patterns, but not in the memory contained in the temporal sequencing of these state vectors. Therefore, we can extend the binary signal transmission scheme to the M-ary

signal case, wherein the multiple stored patterns represent M-ary digits in the considered Hopfield neural networks. Another interesting question is for which type of background noise the Hopfield neural networks are an approximatively optimum receiver for transmitting information-carrying signals and yields a much lower probability of error than that of the matched filter, and which kind of added noise yields the lowest probability of error in this case? In addition, the transmission process of Fig. 1 is a case of synchronized communication. Then, the bit interval T_b at which digits are emitted must be known at the decision, and the state vectors $\mathbf{x}(jT_b)$ are sampled at each end time of bit intervals. Then, if the network dynamics requires a large delay of the convergence of the state vector $\mathbf{x}(t)$ to the correct attraction basin, this decision rule will lead to some wrong bits, and the designed transmission scheme denoted by Fig. 1 needs to be improved. These questions deserve to be further investigated.

References

[1] R. Benzi, A. Sutera, A. Vulpiani, The mechanism of stochastic resonance, J. Phys. A, Math. Gen. 14 (11) (1981) 453–457.

[2] S. Fauve, F. Heslot, Stochastic resonance in a bistable system, Phys. Lett. A 97 (1–2) (1983) 5–7.

[3] B. McNamara, K. Wiesenfeld, R. Roy, Observation of stochastic resonance in a ring laser, Phys. Rev. Lett. 60 (25) (1988) 2626–2629.

[4] L. Gammaitoni, P. Hänggi, P. Jung, F. Marchesoni, Stochastic resonance, Rev. Mod. Phys. 70 (1) (1998) 223–287.

[5] J.J. Collins, C.C. Chow, A.C. Capela, T.T. Imhoff, Aperiodic stochastic resonance, Phys. Rev. E 54 (5) (1996) 5575–5584.

[6] N.G. Stocks, Suprathreshold stochastic resonance in multilevel threshold systems, Phys. Rev. Lett. 84 (11) (2000) 2310–2313.

[7] F. Duan, D. Rousseau, F. Chapeau-Blondeau, Residual aperiodic stochastic resonance in a bistable dynamic system transmitting a suprathreshold binary signal, Phys. Rev. E 69 (1) (2004) 011109.

[8] F. Chapeau-Blondeau, X. Godivier, Theory of stochastic resonance in signal transimission by static nonlinear systems, Phys. Rev. E 55 (2) (1997) 1478–1495.

[9] L. Gammaitoni, M. Martinelli, L. Pardi, S. Santucci, Phase shift in bistable EPR systems at stochastic resonance, Phys. Lett. A 158 (9) (1991) 449–452.

[10] R. Liu, Y. Kang, Stochastic resonance in underdamped periodic potential systems with alpha stable Lévy noise, Phys. Lett. A 382 (25) (2018) 1656–1664.

[11] J. Liu, J. Mao, B. Huang, P. Liu, State observer for stochastic resonance in bistable system, Phys. Lett. A 383 (14) (2019) 1563–1570.

[12] J. Liu, B. Hu, Y. Wang, Optimum adaptive array stochastic resonance in noisy grayscale image restoration, Phys. Lett. A 383 (13) (2019) 1457–1465.

[13] F. Duan, F. Chapeau-Blondeau, D. Abbott, Stochastic resonance in a parallel array of nonlinear dynamical elements, Phys. Lett. A 372 (13) (2008) 2159–2166.

[14] F. Duan, Y. Pan, F. Chapeau-Blondeau, D. Abbott, Noise benefits in combined nonlinear Bayesian estimators, IEEE Trans. Signal Process. 67 (17) (2019) 4611–4623.

[15] D. Schonfeld, On the hysteresis and robustness of Hopfield neural networks, IEEE Trans. Circuits Syst. II, Analog Digit. Signal Process. 40 (11) (1993) 745–748.

[16] M. Riani, E. Simonotto, Stochastic resonance in the perceptual interpretation of ambiguous figures: a neural network model, Phys. Rev. Lett. 72 (19) (1994) 3120–3123.

[17] M. Kawaguchi, H. Mino, D.M. Durand, Stochastic resonance can enhance information transmission in neural networks, IEEE Trans. Biomed. Eng. 58 (7) (2011) 1950–1958.

[18] H. Nishimura, N. Katada, K. Aihara, Deterministic SR phenomena in autoassociative chaotic neural networks, in: International Conference on Neural Information Processing, 2002, pp. 585–589.

[19] H. Mino, D.M. Durand, Enhancement of information transmission of subthreshold signals applied to distal positions of dendritic trees in hippocampal CA1 neuron models with stochastic resonance, Biol. Cybern. 103 (3) (2010) 227–236.

[20] N. Mtetwa, L.S. Smith, Precision constrained stochastic resonance in a feedforward neural network, IEEE Trans. Neural Netw. 16 (1) (2005) 250–262.

[21] A. Karbasi, L.R. Varshney, A. Shokrollahi, A.H. Salavati, Noise-enhanced associative memories, Adv. Neural Inf. Process. Syst. 26 (2013) 1–9.

[22] D. Guo, M. Perc, Y. Zhang, P. Xu, D. Yao, Frequency-difference-dependent stochastic resonance in neural systems, Phys. Rev. E 96 (2) (2017) 022415.

[23] M. Ozer, M. Perc, M. Uzuntarla, Stochastic resonance on Newman-Watts networks of Hodgkin-Huxley neurons with local periodic driving, Phys. Lett. A 373 (10) (2009) 964–968.

[24] M. Perc, Stochastic resonance on weakly paced scale-free networks, Phys. Rev. E 78 (3) (2008) 036105.

[25] R. Benzi, Stochastic resonance in complex systems, J. Stat. Mech. Theory Exp. 2009 (01) (2009) 01052.

[26] G. Pinamonti, J. Marro, J.J. Torres, Stochastic resonance crossovers in complex networks, PLoS ONE 7 (12) (2012) 51170.

[27] S. Haykin, Neural Networks and Learning Machines, Prentice-Hall, Upper Saddle River, NJ, 2009.

[28] J. Hopfield, Neural networks and physical systems with emergent collective computational abilities, Proc. Natl. Acad. Sci. USA 79 (8) (1982) 2554–2558.

[29] R. McEliece, E. Posner, E. Rodemich, The capacity of the Hopfield associative memory, IEEE Trans. Inf. Theory 33 (4) (1987) 461–482.

[30] S.V.B. Aiyer, M. Niranjan, F. Fallside, A theoretical investigation into the performance of the Hopfield model, IEEE Trans. Neural Netw. 1 (2) (1990) 204–215.

[31] S.I. Amari, Mathematical foundations of neurocomputing, Proc. IEEE 78 (9) (1990) 1443–1463.

[32] A.R. Bizzarri, Convergence properties of a modified Hopfield-Tank model, Biol. Cybern. 64 (4) (1991) 293–300.

[33] J. Bruck, On the convergence properties of the Hopfield model, Proc. IEEE 78 (10) (1990) 1579–1585.

[34] E. Cabrera, H. Sossa, Generating exponentially stable states for a Hopfield neural network, Neurocomputing 275 (1) (2017) 358–365.

[35] M. Kobayashi, Multistate vector product Hopfield neural networks, Neurocomputing 272 (2018) 425–431.

[36] M. Kobayashi, Quaternionic Hopfield neural networks with twin-multistate activation function, Neurocomputing 267 (2017) 304–310.

[37] M.F. Danca, N. Kuznetsov, Hidden chaotic sets in a Hopfield neural system, Chaos Solitons Fractals 103 (2017) 144–150.

[38] N. Katada, H. Nishimura, Stochastic resonance in recurrent neural network with Hopfield-type memory, Neural Process. Lett. 30 (2) (2009) 145–154.

[39] V. Pavlovic, D. Schonfeld, G. Friedman, Stochastic noise process enhancement of Hopfield neural networks, IEEE Trans. Circuits Syst. II, Express Briefs 52 (4) (2005) 213–217.

[40] M. Morita, Associative memory with nonmonotone dynamics, Neural Netw. 6 (1) (1993) 115–126.

[41] G.I. Kechriotis, E.S. Manolakos, Hopfield neural network implementation of the optimal CDMA multiuser detector, IEEE Trans. Neural Netw. 7 (1) (1996) 131–141.

[42] I.V. Popova, Y. Ogawa, Application of a modified Hopfield neural network to noisy magnetotelluric data, Izv. Phys. Solid Earth 43 (3) (2007) 217–224.

[43] S. Salcedo-Sanz, R. Santiago-Mozos, C. Bousono-Calzon, A hybrid Hopfield network-simulated annealing approach for frequency assignment in satellite communications systems, IEEE Trans. Syst. Man Cybern., Part B, Cybern. 34 (2) (2004) 1108–1116.

[44] E. Soujeri, H. Bilgekul, Hopfield multiuser detection of asynchronous MC-CDMA signals in multipath fading channels, IEEE Commun. Lett. 6 (4) (2002) 147–149.

[45] S.M. Kay, Fundamentals of Statistical Signal Processing: Detection Theory, vol. 2, Prentice-Hall, Upper Saddle River, NJ, 1998.

[46] S.A. Kassam, Signal Detection in Non-Gaussian Noise, Springer-Verlag, New York, 1988.